

Full paper

Self-powered modulation of elastomeric optical grating by using triboelectric nanogenerator



Xiangyu Chen^a, Yali Wu^{a,b}, Aifang Yu^a, Liang Xu^a, Li Zheng^{b,*}, Yongsheng Liu^b, Hexing Li^{b,*}, Zhong Lin Wang^{a,c,d,**}

^a Beijing Institute of Nanoenergy and Nanosystems, Chinese Academy of Sciences, National Center for Nanoscience and Technology (NCNST), Beijing 100083, China

^b School of Mathematics and Physics, Shanghai Key Laboratory of Materials Protection and Advanced Materials in Electric Power, Shanghai University of Electric Power, Shanghai 200090, China

^c CAS Center for Excellence in Nanoscience, National Center for Nanoscience and Technology (NCNST), Beijing 100190, China

^d School of Materials Science and Engineering, Georgia Institute of Technology, Atlanta, GA 30332-0245, United States

ARTICLE INFO

Keywords:

Triboelectric nanogenerator
Dielectric elastomer
Surface printing technique
Tunable optical grating

ABSTRACT

Tunable optical gratings (TOGs) based on dielectric elastomer actuator (DEA) are combined with triboelectric nanogenerator (TENG), where the actuated strain of DEA under the drive of TENG can regulate the grating period. Hence, a self-powered TOG system can be achieved and TENG can serve as both power supplier and control module for this system. Three different TOG structures have been delicately designed to cooperate with the unique output performance of TENG and the actuated strain of DEA can be utilized to either compress or expand the spacing between grating array. The separation motion of the TENG with a contact surface of 120 cm² can induce a decrease of 16.5% or an increase of 9.4% for the grating period. Both one-dimensional and two-dimensional grating matrixes are designed for the TOG system, while TENG can control two kinds of grating systems to realize several functionalized modulations. The TOG systems based on TENG-DEA conjunction can achieve a fast-speed, highly efficient and multifunctional modulation of the grating period, while the breakdown problem of these TOG devices is largely suppressed since the maximum transferred charges from TENG device is under a limited value. Therefore, the demonstrated self-powered TOG may have tremendous application prospects for various display system, optical sensors, optical communications and so on.

1. Introduction

Tunable optical gratings (TOGs) have great applications in a wide range of fields, including spectroscopic tools, displays, optical sensors, laser switching systems and so on [1–3]. TOGs have commonly been constructed by silicon-based micro-fabrication technology, where the assembled small and rigid elements can be moved independently by mechanical actuation, and thus the grating period as well as the diffraction angles can be changed accordingly. However, most TOGs relied on standard hard materials usually have very limited tuning range [4]. Even though it is possible to achieve a change of the grating period up to 25% through the high precision MEMS technology, this kind of device still suffers from the slow response and high power loss [5]. Therefore, another promising approach for efficient TOG devices based on soft membranes and dielectric elastomer actuators (DEAs)

has been intensively studied [6–9]. The diffraction performance of soft elastomeric TOGs may be not as precise as those based on hard materials. Nevertheless, they can offer many unique advantages, such as the large and continuous tuning range, low fabrication cost and fast response speed. And more importantly, the rapid emergence of various stretchable electrode materials and the development of nano fabrication techniques [10,11], not only promote the innovation of DEA devices, but also bring forth many possibilities to modify the DEA-based TOGs systems.

On the other hand, self-powered nanosystems by using triboelectric nanogenerator (TENG) as energy supplier are receiving more and more attentions due to their huge application prospects in portable/wearable electronics, Micro-Electro-Mechanical System (MEMS) and human-machine interfacing [12–16]. TENG can directly convert various mechanical motions into electrical energy and its superior character-

* Corresponding authors.

** Corresponding author at: Beijing Institute of Nanoenergy and Nanosystems, Chinese Academy of Sciences, National Center for Nanoscience and Technology (NCNST), Beijing 100083, China.

E-mail addresses: zhengli@shiep.edu.cn (L. Zheng), Hexing-li@shnu.edu.cn (H. Li), zlwang@gatech.edu (Z. Lin Wang).

<http://dx.doi.org/10.1016/j.nanoen.2017.05.039>

Received 21 April 2017; Received in revised form 14 May 2017; Accepted 16 May 2017

Available online 25 May 2017

2211-2855/ © 2017 Elsevier Ltd. All rights reserved.

istics of strong adaptability, flexible structure design and environmental friendliness can support this technique to work for a lot of multi-functional nanosystems [17–19]. The contact or tribo motion of TENG can instantaneously generate a high electrostatic field, which allows TENG to serve as high voltage source to drive or control some smart electromechanical systems [20–22]. For example, the DEA based on stretchable insulating elastomers has been proved to be a good enabling technique to work with TENG and the TENG-DEA conjunction systems have demonstrated a series of practical applications in the field of artificial muscle, self-powered wearable electronics and so on [20,21]. All these progresses inspired us to design a self-powered TOG system based on TENG-DEA technology, which can further popularize the application of TENG technique in the field of applied optics. Unfortunately, the operation voltage for the DEA elements in TOG system is usually a few thousands volts, which is a potential threat to the peripheral devices and to the TOG itself. However, the output voltage from TENG can meet DEA's crucial demand for high driving voltage, because the limited amount of output charges from TENG can automatically inhibit the possibility of electrical breakdown in this TOG system. Therefore, the conjunction of TENG and DEA-based TOGs technique can fully develop the advantages of both techniques and thus open up many new research fields. However, it is worth noting that the output capability of TENG is not exactly equal to the commercial power source. Therefore, the previously reported soft TOGs [6–9], which rely on the actuation from the electrically powered DEA, may not be the optimized device for TENG-based system. To realize an effective manipulation of the TOGs, it is necessary to design some special

TOG systems intentionally to fit the unique output performance of TENG.

In this study, we have demonstrated a concept of motion-modulated TOGs based on the TENG-DEA conjunction system. The tunable optical grating array is directly made by printing the elastomer film on the master grating with aggregated metallic nanoparticles covered on its surface. The fabricated gratings show almost no increase in the stiffness of the elastomer film and thus the deformation of the TOG can be actuated by a rather small voltage signal, which is quite suitable for the TENG-based system. In order to achieve an effective modulation of the diffraction effect, three different transmission type of TOGs have been designed for either compressing or expanding the grating array. All these TOGs are designed to fit the output capability of the TENG and a simple contact-separation motion can be used to regulate the grating period. This self-powered TOGs can promote the applications of TENG in the fields of laser based systems or display device. With the consideration of excellent human/machine interactive capability of TENG, this motion-modulated TOGs can also serve as a fundamental element for optical communication systems or various optical sensors.

2. Results and discussion

Fig. 1a shows the basic structure and operation principle of TENG-DEA conjunction system. A single-electrode TENG using contact-separation motion mode was employed as the driving element for the conjunction system, which is similar to our previous study [20]. For this TENG-DEA conjunction system, the tribo-induced charges are

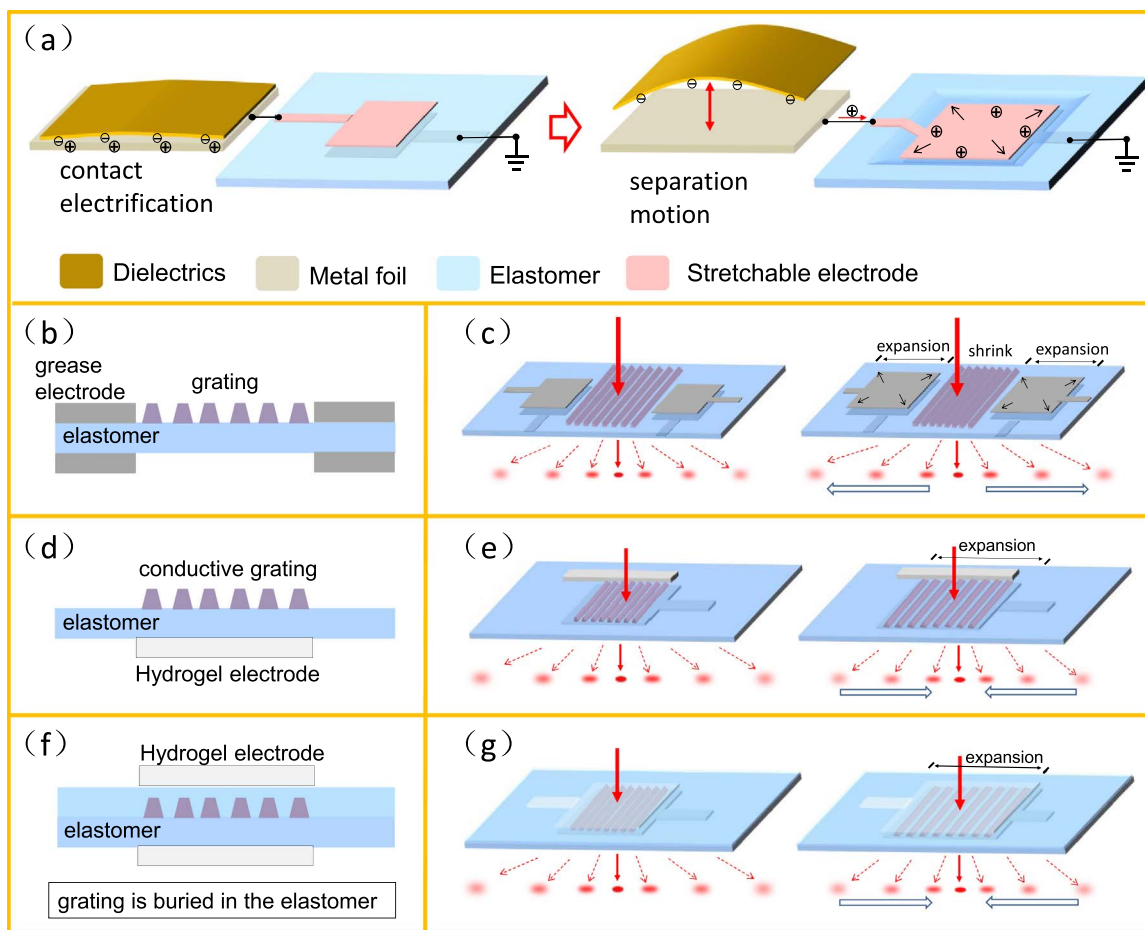


Fig. 1. a) The basic structure and the operation principle of TENG-DEA conjunction system, where a single-electrode TENG using contact-separation motion mode was employed as the driving element for the conjunction system. b) The structure design of the compression mode TOGs, c) the working principle of the compression mode TOGs, d) the structure design of the TOGs with expansion mode 1, e) the working principle of the TOGs with expansion mode 1, f) the structure design of the TOGs with expansion mode 2, g) the working principle of the TOGs with expansion mode 2.

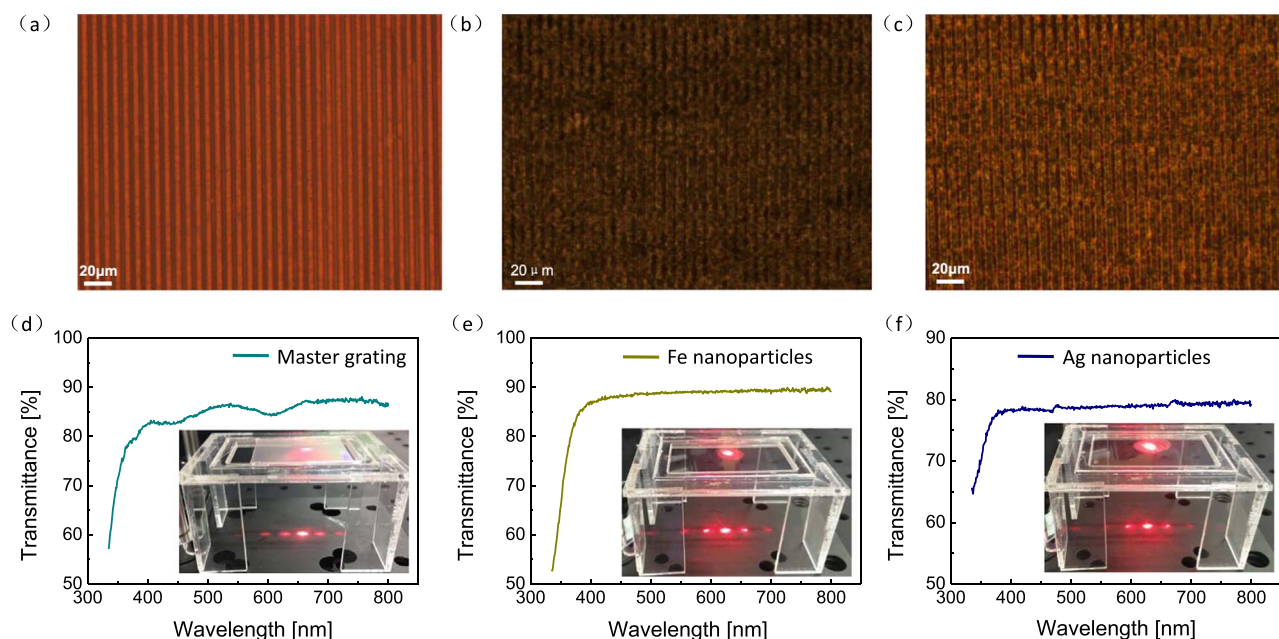


Fig. 2. The micrograph of the different grating for a) master grating ; b) Fe nanoparticles ; c) Ag nanoparticles. The transparency of different gratings and photograph (Inset) of laser diffraction performance for a) master grating ; b) Fe nanoparticles ; c) Ag nanoparticles.

generated by the DEA device and the internal capacitor of the TENG. The internal capacitance of the single-electrode is a rather small value and it will not change with different motion position, which means large amount of tribo-charges are occupied by the DEA device. Hence, an efficient and reliable operation of DEA device can be achieved and that is the reason for us to usually choose single-electrode TENG for operating TENG-DEA conjunction system. The contact-electrification process happens between dielectric layer (Kapton) and Al foil, where positive (negative) charges are left on the Al foil (Kapton film). The contact-separation motion of the TENG applies a strong electric field on the DEA, which can induce a strong Maxwell stress between two electrodes of DEA, and the stretchable electrodes as well as the elastomer film show expansion deformation under this Maxwell stress. The Maxwell stress can be given as: $P = -\epsilon E^2$, where E is the electrical field and ϵ is the permittivity of the elastomer layer [23]. Here, the contact-separation motion of the TENG has the dual function as both the power supply and the control signal for the deformation of the DEA. The separation motion of Kapton film triggered the actuation of the DEA, where the elastomer film connected between Al foil and the ground endures the tribo-generated electrostatic field owing to its capacitance characteristics. Based on the fast response of the elastomer, the mechanical strain of the DEA will be activated immediately after the separation motion. After that, as soon as the Kapton film returns to the original position, the charge neutralization process happens between Al foil and Kapton film and accordingly the potential drops as well as the strain on the elastomer relaxes. This is the basic operation process of the TENG-DEA system. Based on this operation principle, the DEA elements in the TOGs systems can be used to control the deformation of the TOG while the output voltage from TENG can serve as the power supply. As shown in Fig. 1(b, c), Fig. 1(d, e) and Fig. 1(f, g), three kinds of TOG structure (compression mode, expansion mode 1 and expansion mode 2) are fabricated for the study, respectively.

The compression mode TOG is consisted of two DEA elements and a grating arrays (see Fig. 1(b, c)) [6,7]. The grating array in this case is made of aggregated metallic nanoparticles. The operation principle for this compression mode TOG is schematically illustrated in Fig. 1c. Two DEA elements with silicon/carbon grease as electrodes are fabricated on one piece of elastomer film and the grating array is printed on the spacing region between two DEA devices. The elastomer film is

constrained by the boundary frames so that the induced strain is concentrated passively in the middle part. The pre-strain ratio of 600% is applied on the elastomer film before the printing of this grating array, where the influence of softness of the elastomer film caused by the nanoparticle gratings is negligible. The actuation from TENG leads to the expansion of two stretchable electrodes, while compressive strain is generated in the passive region at the same time and thereby the period of grating in the middle part is reduced. In order to further study this self-powered optical modulation technique, we further designed two novel structure of expansion mode for TOG besides this compression mode. Fig. 1(d, e) show the structure and operation principle of the expansion mode 1. In this TOG system, the conductive Ag nanoparticle is used for fabricating the grating array and thus the grating array itself can also serve as one electrode for the DEA element. A transparent hydrogel film is employed as the other electrode in the back and the elastomer film is sandwiched between the grating electrode and the hydrogel electrode. The transparency of the hydrogel is about 95% and accordingly an almost transparent type of TOGs can be prepared. Under the drive of the output voltage from TENG, the hydrogel electrode as well as the grating array expands due to the existence of Maxwell stress, which is similar to the operation of common DEA device. The expansion of grating arrays leads to the increase of the grating period and therefore a self-powered TOG for increasing the grating period can be achieved. It is also necessary to point out that the tensile property of this conductive grating array is not favorable in experiment. Thus, the expansion strain of the device may not be high enough to realize an effective operation of the device. In this case, we further proposed expansion mode 2, as illustrated in Fig. 1(f, g). After the grating arrays are printed on the pre-strained elastomer film, PDMS is spin-coated on top of grating arrays with a thickness of 100 μm and accordingly, the grating arrays are sealed by PDMS film. Then, two hydrogel electrodes are stuck on both top and bottom side of the sealed grating arrays, as shown in Fig. 1f. The hydrogel electrodes will not blur the grating pattern due to the protection from PDMS film. This new design of TOG can fully utilize the transparency and stretchability of hydrogel electrodes. Accordingly, the fabricated device can work as a common DEA device, where the actuation from TENG results in the expansion of both the elastomer film and the grating arrays. The hydrogel electrodes and the elastomer are soft enough to show rather larger deformation, which ensure an

effective modulation of TOG.

The grating array is directly printed on the surface of elastomer film due to the sticky characteristics of the elastomer itself. A master grating is employed as the plate for printing and the micrograph picture of the grating structure is shown in Fig. 2a, where the grating period is about 8 μm . The metallic nanoparticles are homogeneously dispersed on the surface of the master grating. After that, the master grating covered by nanoparticles is pressed on the surface of the pre-strained elastomer film (VHB 9473) and a precise linear motor can be used to guide the motion of this grating. The nanoparticles on the master grating can be automatically attached on the sticky surface of the elastomer film and the grating array thus can be formed on the surface of the elastomer film. The clarity of the printed grating can be controlled by changing the amount of nanoparticles dispersed on the master grating. Different kinds of metallic nanoparticles have been tested for this fabrication process. The Fe and Ag nanoparticles can both achieve good grating arrays on the elastomer film. The micrograph picture of these two kinds of grating array (Fe and Ag) is shown in Figs. 2b and 2c, respectively. Meanwhile, the enlarged pictures of the edge of the printed grating are shown in Fig. S1a and S2b. The Fe nanoparticles are good insulator since it is easy to be oxidized in the air, while the Ag nanoparticles can form some conductive arrays if the thickness of the grating increase to a certain value. For the compression mode and expansion mode 2, the grating array is made by Fe nanoparticles. For expansion mode 1, the conductive grating arrays are necessary to serve as the electrode and thus the Ag nanoparticles are employed for fabricating the grating arrays. We have also tried other nanomaterials for printing the grating arrays. The printed grating by using carbon and Au nanoparticles can be seen in Fig. S1c and S1d in the supporting info. The printed grating

array cannot show clear optical diffraction behavior. The carbon nanoparticles are too light and soft, while the Au nanoparticles tend to agglomerate together. Neither of them can clearly duplicate the grating pattern on the master plate. So far, Fe and Ag nanoparticles are preferred for printing the grating arrays. The optical transmittance data at all wavelength for three different samples (master grating, Fe nanoparticles and Ag nanoparticles) are shown in Fig. 2d-f. In order to maintain the conductivity of the grating arrays, the thickness of the Ag gratings needs to be increased. Hence, the Ag grating arrays have lower transmittance compared with the grating arrays based on Fe nanoparticles. The replication accuracy of these gratings is slightly deteriorated by the sparsed nanoparticles. However, this nanoparticle based gratings are the best candidates to work with TENG since they hardly increase the stiffness of the elastomer film and the flexibility of this printing method also largely simplified the fabrication process of the TOG system.

For the operation of the prepared TOGs, the output signal from single-electrode TENG, which is driven by a digital linear motor, is directly applied on the TOG devices without any auxiliary circuits or transformer module. Hence, a fully self-powered TOG system can be achieved, where mechanical motion can serve as both power source and control signal by use of a TENG. During the performance measurements of the TOG, the top plate of TENG are controlled by a linear motor in the vertical direction of the bottom plate, while the bottom plate is fixed on a stable stage. The tribo materials are selected as Kapton film and Al foil, which are attached on the bottom and top plate, respectively. At the initial state, two plates are aligned with each other and the separating displacement of the top plate can be controlled by the linear motor with a position resolution of 1 mm.

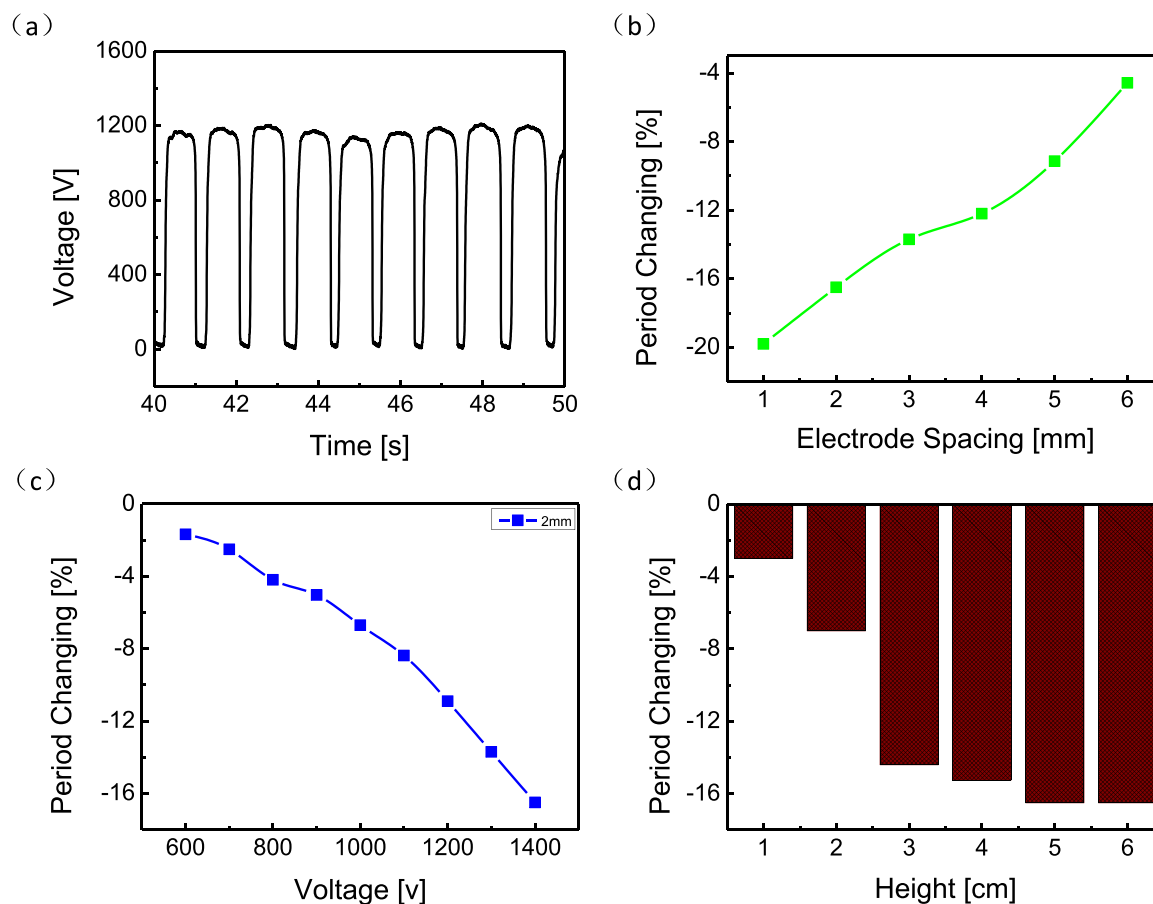


Fig. 3. The performance measurement of the TOG based on compression mode, (a) output voltage from TENG to TOG under contact-separation motion, (b) the highest period changing of the grating under the drive of the same TENG, where the electrodes spacing is changing from 1 mm to 6 mm, (c) TOG under the drive of the stable voltage and the electrodes spacing is 2 mm, (d) the relationship between changing of the grating period and separation height of the TENG.

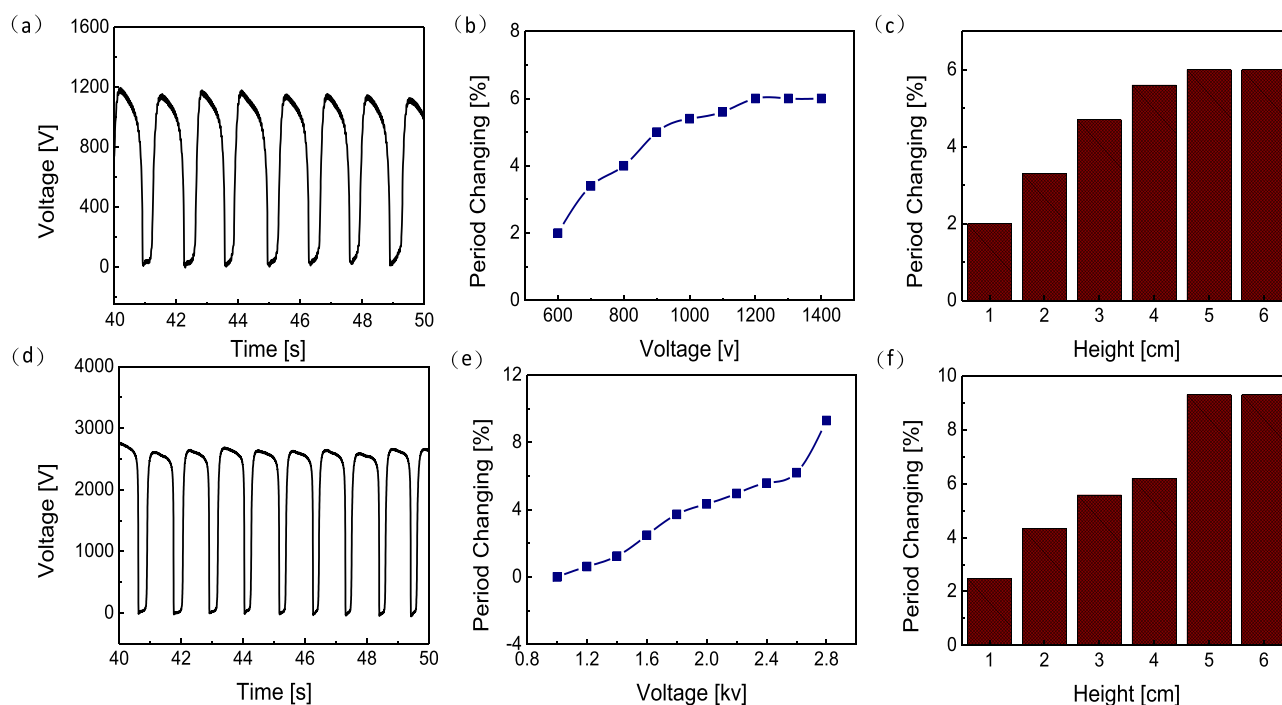


Fig. 4. The performance measurement of the TOG based on expansion mode 1 and expansion mode 2, a) output voltage from TENG to TOG (expansion mode 1), b) TOG under the drive of the stable voltage (expansion mode 1), c) the TOG under the drive of the TENG (expansion mode 1), (d) output voltage from TENG to TOG (expansion mode 2) (e) TOG under the drive of the stable voltage (expansion mode 2) (f) the TOG under the drive of the TENG (expansion mode 2).

The separating movement is in a symmetric acceleration–deceleration mode with an acceleration rate of $\pm 20 \text{ m s}^{-2}$ and the velocity can be changed optionally by a control system. In order to demonstrate the output performance of the TENG device, the maximum transferred charges (Q_{sc}) and the short-circuit current (I_{sc}) under the highest velocity of the motor ($\approx 1 \text{ m s}^{-1}$) are both recorded by an electrometer with a very high internal resistance, as shown in Fig. S2a and S2b. In this experiment, the dynamic performance of the output voltage is measured by a modified electrostatic voltmeter (Monroe ME-297). The Monroe ME-297 voltmeter has a very high internal resistance, which can help to maintain the tribo-induced charges from TENG, and its effective range is from 0 V to 3500 V. Hence, the open-circuit voltage of the TENG is measured to be about 3000 V (see Fig. S2c). It is important to note that the real output voltage from TENG may be even higher than the value, since the leakage phenomenon may still exist in the ME-297 voltmeter. As demonstrated in our latest paper [22], the electrostatic actuator, which can only be operated under a voltage source larger than 3500 V, can be easily driven by a palm-sized TENG. However, this generated V_{oc} from TENG is a static value under the isolated condition, which will be decreased quickly if the electrostatic isolation is disturbed. It is also necessary to design some strategy to erase offsets of the output voltage of TENG. The detailed control strategy of the TENG-DEA system is studied in our previous work [21]. In this self-powered TOG system, the TENG simultaneously drives the deformation of both two DEA devices in the system, as illustrated in Fig. 1c. The output voltage from TENG is applied on one electrode of each DEA with the other electrode grounded, as shown in Fig. 1a. The generated voltage drop on the DEA is determined by the resistivity of the devices and the output voltage from TENG gradually decreases with the decrease of the resistivity. As shown in Fig. 3a, the maximum voltage drop on the TOGs generated by TENG is detected to be 1200 V, suggesting that the DEA devices in this TOG system have some charge leakage and thus the output voltage is decreased in comparison with the open-circuited condition. As can be seen in Fig. 1b, the grating array is located in the passive region between two DEA devices. The electrode spacing between two DEA devices is a critical parameter for determining the performance of TOG. The maximum period changing

of the TOG under the drive of TENG is recorded in Fig. 3b, where the electrode spacing is changing from 1 mm to 6 mm. The decrease of the electrode space leads to the enhancement of the tunability of the grating period. However, if the electrode spacing is too small, the laser spot will be partially blocked. Therefore, the optimized electrode spacing in this experiment is around 2 mm. For the compression mode TOG with an electrode spacing of 2 mm, the induced period changing under the different applied voltage can be seen in Fig. 3c. The highest period changing is -16.5% under the applied voltage of 1400 V, while the breakdown voltage of this TOG device is about 1500 V. Meanwhile, the separation distance of TENG can be used to regulate the actuation behavior of the DEA, which has been demonstrated in our previous studies [20]. Fig. 3d shows the actuated period changing of TOG under the control of the contact-separation motion. Here, the separation velocity is 1 m s^{-1} and the separation height is gradually changed from 1 cm to 6 cm. After the separation height reaches 5 cm, the further increase of the height cannot change the period of the grating, which is decided by the edge effect of the TENG [24,25]. The largest period changing under the actuation of TENG also can reach -16.5% with a contact area of 120 cm^2 . This compression mode can only decrease the grating period of TOG and the diffracted laser spots are moving outward (see Movie 1 in supporting info). It is necessary to design some other TOG systems that can also control the expansion of the grating arrays, in order to fully demonstrate this proposed concept of self-powered TOGs.

Supplementary material related to this article can be found online at [doi:10.1016/j.nanoen.2017.05.039](https://doi.org/10.1016/j.nanoen.2017.05.039).

The TOG based on expansion mode 1 and expansion mode 2 (see Movie 2 and Movie 3 in supporting info) are experimentally studied by using the same TENG device and the results are displayed in Fig. 4. For expansion mode 1, the thickness of the elastomer film is the same as the compression mode and only the two electrodes are replaced by Ag nanoparticles and the hydrogel, respectively, as can be seen in Fig. 1d. Accordingly, the generated voltage drop on this TOG is about 1250 V, which is comparable with that in compression mode. The actuated period changing of the grating under the drive of both voltage source and TENG are shown in Figs. 4b and 4c, respectively. The largest

changing of the grating period is up to an increase of 6.1%. The grating arrays made of Ag nanoparticles can function as the electrode in DEA device. While its conductivity can be enhanced by increasing the clarity and the thickness of the arrays, the stretchability of this grating electrode cannot be increased easily. Therefore, the actuated period changing of this TOG can not be high enough. However, it is necessary to report this structure due to its novel and facile fabrication method. The dual function of this grating arrays as both optical element and electrode is a novel concept and it can be probably applied in the research filed of optical metasurface for light trapping or vector beam propagation. Fig. 4d shows the output voltage from TENG working on the TOG with expansion mode 2. The generated voltage drop on the TOG is about 2500 V, which is closer to the V_{oc} value from TENG in comparison with other two kinds of samples. The spin-coated PDMS film increases the thickness of the whole TOG and the good insulating performance of PDMS also significantly suppresses the leakage phenomenon through the TOG. The increase of the resistivity of the device leads to the increase of the established voltage drop. Meanwhile, for expansion mode 2, the period changing of the TOG under the drive of both voltage source and TENG are measured separately and the results are shown in Figs. 4e and 4f. The breakdown voltage of the device is about 2800 V and the largest changing of the grating period is up to an increase of 9.4%, which has been improved about 50% comparing with expansion mode 1 (see Fig. 4e). This tunability can be further improved, since there are several ways to increase the breakdown voltage of the hydrogel based DEA devices. The output voltage from TENG can also drive the TOG to show a period changing of 9.4%, while the separation height can be used to control the period changing, as can be seen in Fig. 4f. For all these three working modes, the output energy from TENG is enough to actuate the TOG to show notable deformation, demonstrating an effective manipulation of the TOG system. On the other hand, there is almost no breakdown phenomenon happened with the TOG driven by TENG. The generated tribo-charges from TENG is a limited value and the maximum amount of transferred charges is only 370 ~ 390 nC (see Fig. S2a). When the applied voltage on the elastomer film is close to its breakdown threshold, the charge leakage phenomenon becomes significant. Accordingly, the tribo-generated charges will

be quickly consumed due to the current leakage and the voltage drop on the DEA devices cannot be further increased [21]. This mechanism can automatically protect the DEA sample and the TOG system. Therefore, the probability of electrical breakdown is negligible under the drive of TENG, indicating a much safer and effective operation of the TOG.

Supplementary material related to this article can be found online at [doi:10.1016/j.nanoen.2017.05.039](https://doi.org/10.1016/j.nanoen.2017.05.039).

The printed grating arrays based on metallic nanoparticles is a simple but effective method to fabricate soft TOG system. In order to further explore the applicability of this TENG-based TOG technique, we prepared a two dimensional (2D) grating matrix based on metallic nanoparticles and also demonstrated the capability of TENG-DEA conjunction for manipulating the 2D TOG system. The structure and working principle of these 2D TOG systems are graphically illustrated in Fig. 5. Fig. 5a is the 2D TOG system based on compression mode. The grating arrays are printed on both top and bottom side of the elastomer film by using Fe nanoparticles, where two grating arrays are in vertical cross structure. This double-layer grating can induce a matrix of laser spots on the projection plane through diffraction effect, as can be seen in Fig. 5a, and the actuation from the TENG leads to the expansion of two DEA elements on the same elastomer film. Accordingly, the diffracted laser matrix on the projection plane moves outward in X-axis and moves inward in Y-axis, as can be seen in Fig. 5a. This is the compression mode for 2D TOGs, where TENG performs two kinds of modulation on the same TOG devices. The 2D TOG system based on expansion mode 2 is another design of the sample, as shown in Fig. 5b. Here, two PDMS film is spin-coated on both top and bottom side of the elastomer film and the double-layer grating arrays are sealed by PDMS. Two hydrogel electrodes are attached on both sides of the sealed grating arrays, which is similar to Fig. 1f. The expansion of the hydrogel electrodes results in the expansion of the grating and the diffracted laser matrix move inward in both X-axis and Y-axis direction. The photograph of the diffraction effect of this double-layer grating is shown in Fig. 6a. The demonstration video of these 2D TOG systems can be found in Movie 4 in supporting info. For the 2D TOG based on the compression mode (see

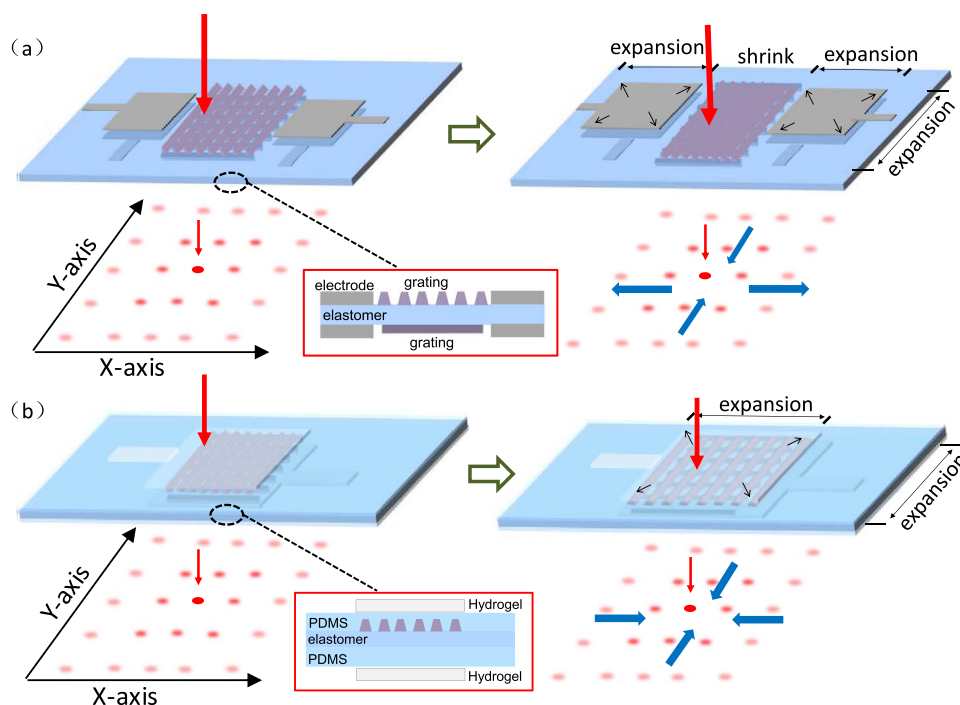


Fig. 5. Further demonstration of self-powered TOG technique with 2D grating system. Both (a) compression mode and (b) expansion mode 2 are applied for manipulating the deformation of these 2D TOGs.

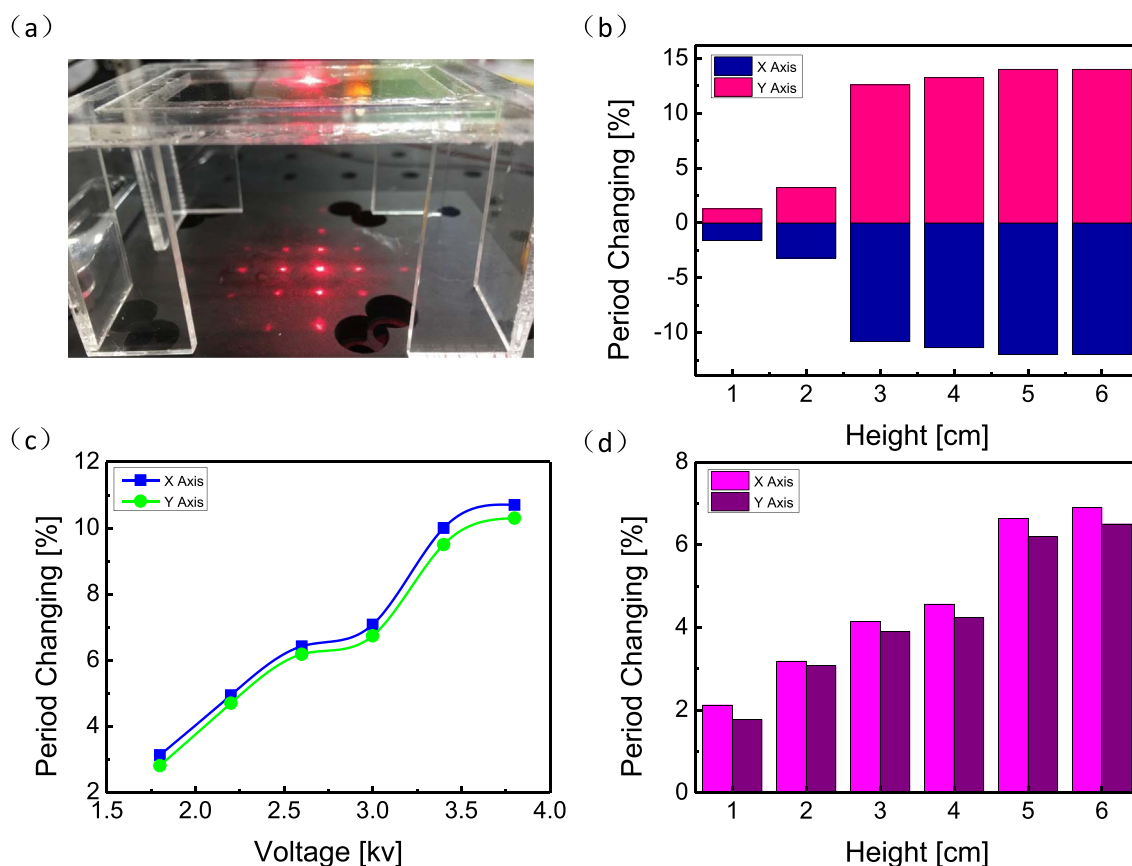


Fig. 6. The performance measurement of the 2D TOG system. a) The photograph of the 2D diffraction matrix. b) For the compression mode TOG, the induced changing of the grating period under the drive of TENG. The grating period in the horizontal direction (X-axis) will be decreased, while the grating period in the vertical direction (Y-axis) will be increased. c) For the expansion mode 2, the induced changing of the grating period under the drive of the voltage source. Here, both the grating period in the horizontal direction (X-axis) and the vertical direction (Y-axis) will be increased. b) The induced changing of the grating period under the drive of the TENG (expansion mode 2).

Fig. 5a), the modulation of the 2D laser matrix under the drive of TENG is summarized in Fig. 6b. With the increase of the separation height, the grating period on two directions (X-axis and Y-axis) starts to change. The largest changing percent of the grating period in X-axis is -12% (decrease), while that in Y-axis is 14% (increase). The period changing in X-axis is slightly decreased in comparison with the single-layer grating's case (see Fig. 3d). It is possible that the repeated printing processes may cause some change to the mechanical performance of the elastomer. The 2D TOGs based on expansion mode 2 are also measured, where the TOGs system is driven by both voltage source and TENG. Fig. 6c shows the period changing of 2D TOG (expansion mode 2) under the drive of voltage source. The final period changing under the breakdown voltage of 3800 V is about 10.7% in X-axis and 10.2% in Y-axis, respectively. The multilayer structure of this 2D TOG (see Fig. 5b) strongly increase the thickness and the resistance of the TOGs, which need the increase of the operation voltage. Meanwhile, the stiffness of the PDMS film also influence the actuation performance of the TOGs. Accordingly, for the same sample (expansion mode 2) under the drive of TENG, the changing percent of the grating period in X-axis and Y-axis are 6.9% and 6.5% , respectively, as shown in Fig. 6d. The V_{oc} from TENG is measured to be 3000 V, which is already not enough to completely drive this 2D TOG. These results can also explain why the nanoparticles based grating, which hardly increases the thickness and the stiffness of the device, is quite suitable for this self-powered TOGs. To solve this problem, we could either use the same TENG device with larger size of tribo-surface or employ some more efficient surface modification method, such as corona polarization technique, to further promote the output capability of TENG. The demonstration of these 2D TOG systems in Fig. 6 reveals the flexible maneuverability of the printing method based on metallic nanoparti-

cles and also enriches the functional study of the elastomeric TOG devices.

Supplementary material related to this article can be found online at [doi:10.1016/j.nanoen.2017.05.039](https://doi.org/10.1016/j.nanoen.2017.05.039).

The grating arrays in the above studies are all stripe gratings, which are printed from the same master grating. Since the printing technique based on nanoparticles is a universal method for copying the nano/micro patterns, dot-matrix gratings instead of stripe gratings can also be printed on the surface of elastomer film by using this method, which is an easier way to realize a 2D grating matrix. The design of TOG based on dot-matrix grating is shown in Fig. 7a, where two pairs of DEA elements (A and A', B and B') are located around the dot-matrix. In Fig. 5a, for the compression mode TOG with only two DEA elements, the expansion of the DEA electrode lead to the compression of the grating arrays in the X-axis direction and the expansion of the grating arrays in the Y-axis direction. In order to further enhance the deformation of the grating arrays in the X-axis direction, the unnecessary expansion strain in the Y-axis direction should be restrained and the actuation force from DEA element can focus on the X-axis direction. Hence, as shown in Fig. 7a, the two DEA elements in the Y-axis (B and B') is used to restrain the expansion of the grating matrix and larger compression strain can be achieved in the X-axis direction. Here, the electrode spacing between two DEA elements on both X-axis and Y-axis direction is fixed to 6 mm. The photograph of the TOG devices and the performance of the diffraction can be found in Fig. 7b, while the micrograph of the dot-matrix gratings can be seen in Fig. 7c and each dot in the matrix is a square with a width of $10\ \mu\text{m}$. This dot-matrix TOG under the drive of the voltage source are studied, as can be seen in Fig. 7d and the Movie 5 in the supporting info. The largest period changing can reach 24.5% and the driving voltage for this kind

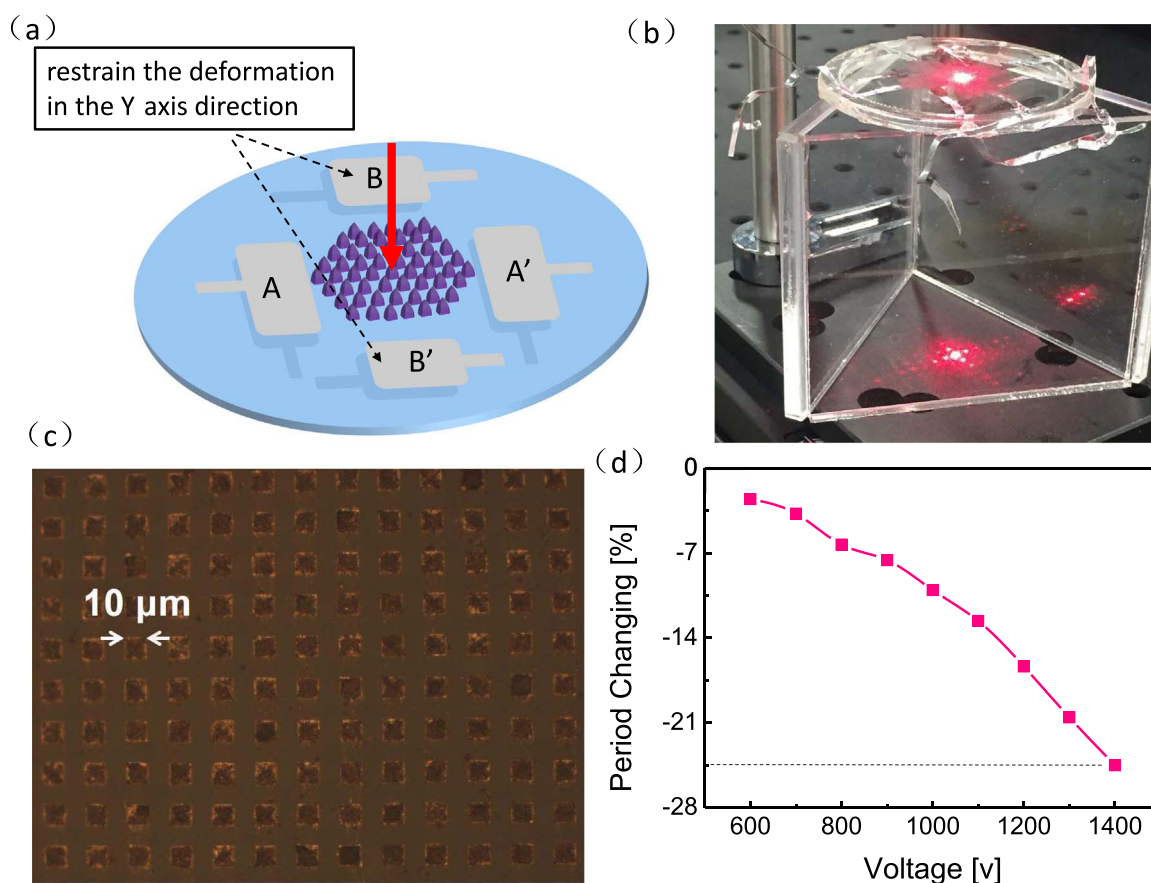


Fig. 7. The nanoparticle based grating can also be used for printing the dot matrix gratings, a) the design of the TOG based on the dot matrix grating, electrodes of B and B' are placed for restraining the deformation in Y-axis direction, b) the photograph of the TOG device, c) the micrograph of the dot matrix on the surface of the elastomer, which is assembled by nanoparticles, d) the changing of the diffraction performance under the drive of applied voltage, where the spacing between each electrode pairs is 6 mm.

of deformation is only 1500 V. It is worth to note that the driving voltage for this kind of TOG device in the previous study is at least two or three times larger than our sample [6–8], indicating a very efficient operation of the TOG by TENG. This additional experiment demonstrates the advanced operating capability of this TOG system, not only for the conjunction study with self-powered TENG, but also for the common applications in the electrically powered system.

Supplementary material related to this article can be found online at [doi:10.1016/j.nanoen.2017.05.039](https://doi.org/10.1016/j.nanoen.2017.05.039).

3. Conclusions

In summary, by utilizing the controllable deformation strain generated in TENG-DEA system, we have demonstrated a concept of self-powered TOGs. Three different TOG structures have been designed to work with TENG-DEA system, where the deformation strain of the DEA elements can either increase or decrease the grating period. We can simply maneuver a single-electrode TENG with a contact surface of 120 cm² to modulate the grating period to a decrease of 16.5% or an increase of 9%. The printing method based on metallic nanoparticles used to fabricate the grating arrays for the TENG-based TOG system is quite simple and facile, since it hardly increases the stiffness of the elastomer film. Both stripe gratings, double-layer gratings and dot-matrix gratings are printed on the elastomer film to realize 1D and 2D diffraction matrix under the control of TENG to perform functionalized modulation. The TENG-based TOG systems have superior characteristics of fast response speed, large tunable range and low fabrication cost, while the possibility of electrical breakdown of the TOG is negligible under the drive of TENG due to the limited tribo-charges. Hence, this proposed technique can serve as a fundamental element for

display system, optical sensors or optical communication systems. The design and the concept of this self-powered TOG system has great potential in the application of functional metasurface and in the development of the possible applications of TENG in light trapping or vector beam propagation.

4. Experimental sections

4.1. Design and measurement of single-electrode TENG

The single-electrode TENG designed in our experiment has a common structure with two plates to perform the contact and separation motion. The detailed design can be seen in previous paper [20]. The Al foil with rectangular shape (12 cm × 12 cm) was selected as one of tribo-surface and the output electrode. The dielectric film is a Kapton adhesive tape (thickness ≈ 50 μm, 10 cm × 12 cm). The inductively coupled plasma (ICP) reactive-ion etching process is performed on the surface of Kapton tape, in order to achieve nano-patterned structures [20]. This single-electrode TENG was driven by a numerical controllable linear motor during the measurements, where the sliding distance and the motion speeds can be controlled by the monitoring circuits, and the two plates are kept in intimate contact at the beginning. The voltage output performance was measured by a Monroe ME-297 electrometer, while the transferred charges and the current were measured by Stanford Research Systems Keithley 6514.

4.2. Fabrication and measurement of TOG system

The self-powered TOG system is based on the grating array and TENG-DEA elements. The grating array is directly printed on the

surface of elastomer film by using the metallic nanoparticles. A master grating is employed as the plate and the metallic nanoparticles are homogeneously dispersed on the surface of the master grating (area size is $3\text{ cm} \times 3\text{ cm}$). The dispersed amount of Fe nanoparticles is about 150 mg and the amount of Ag nanoparticles is about 250 ~ 300 mg. After that, the master grating covered by nanoparticles is pressed on the surface of the pre-strained elastomer film (VHB 9473) and the nanoparticle arrays can be attached on the sticky surface of the elastomer film. The micrograph pictures of the grating structure are captured by microscope (ZEISS, Imager. M2m). The area ratio of the pre-strain for the elastomer film is 600% [20]. This printing technique can be used to duplicate both the stripe gratings, the double-layer gratings and the dot-matrix gratings. The DEA elements are used to regulate the deformation of the grating and three different TOG structures have been designed. The changing of the grating period can be calculated from the change of the diffraction angle by using grating equations [26]. A laser beam with the wavelength of 632 nm is applied on the grating in the vertical direction, while the distance between grating and the projective plane is fixed. The motion of the diffracted laser spot on the projective plane is recorded by a fixed high-speed camera (PHOTRON, AX200) and thus the changing of the diffraction angle can be calculated by using trigonometric relations.

4.3. Fabrication of DEA elements

The DEA element in the TOG system is consisted of two stretchable electrodes and the elastomer film sandwiched between two electrodes. Both silicon/carbon grease and the hydrogel are employed as the electrode materials. The synthesis process can be found in the previous studies [27].

Acknowledgements

This work was supported by the National Key R & D Project from Minister of Science and Technology (2016YFA0202704), the “thousands talents” program for pioneer researcher and his innovation team, China, NSFC Key Program (No. 21237003) and National Natural Science Foundation of China (Grant Nos. 2016YFA0202704, 61405131, 51432005, 11674215, 5151101243, 51561145021), Shanghai Pujiang Program (No. 16PJ1403500), “Shu Guang” project of Shanghai Municipal Education Commission (No. 13SG52), Science and Technology Commission of Shanghai Municipality (Nos. 14DZ2261000).

Appendix A. Supplementary material

Supplementary data associated with this article can be found in the online version at [doi:10.1016/j.nanoen.2017.05.039](https://doi.org/10.1016/j.nanoen.2017.05.039).

References

- [1] S.C. Truxal, K. Kurabayashi, Y.-C. Tung, *Int. J. Optomechatronics* 2 (2) (2008) 75–87.
- [2] G.T. Paloczi, Y. Huang, A. Yariv, J. Luo, A.K.Y. Jen, *Appl. Phys. Lett.* 85 (2004) 1662–1664.
- [3] G. Huang, J. Shin, W. Lee, T. Park, W. Chu, M. Oh, *Opt. Express* 23 (2015) 21090–21096.
- [4] M. Kollosche, S. Döring, J. Stumpe, G. Kofod, *Opt. Lett.* 36 (8) (2011) 1389–1391.
- [5] Y.S. Yang, Y.H. Lin, Y.C. Hu, C.H. Liu, *J. Micromech. Microeng.* 19 (1) (2008) 015001.
- [6] M. Aschwanden, A. Stemmer, *Opt. Lett.* 31 (2006) 2610–2612.
- [7] G. Kofod, D.N. McCarthy, J. Krissler, G. Lang, G. Jordan, *Appl. Phys. Lett.* 94 (2009) 202901.
- [8] M. Kollosche, S. Döring, J. Stumpe, G. Kofod, *Opt. Lett.* 36 (2011) 1389–1391.
- [9] L. Maffli, S. Rosset, M. Ghilardi, F. Carpi, H. Shea, *Adv. Funct. Mater.* 25 (11) (2015) 1656–1665.
- [10] C. Keplinger, J.Y. Sun, C.C. Foo, P. Rothemund, G.M. Whitesides, Z. Suo, *Science* 341 (2013) 984–987.
- [11] X. Chen, X. Pu, T. Jiang, A. Yu, L. Xu, Z.L. Wang, *Adv. Funct. Mater.* 27 (2017) 1603788.

- [12] Z.L. Wang, *ACS Nano* 7 (2013) 9533–9557.
- [13] Y. Hu, Y. Zhang, C. Xu, L. Lin, R.L. Snyder, Z.L. Wang, *Nano Lett.* 11 (6) (2011) 2572–2577.
- [14] G.T. Hwang, H. Park, J.H. Lee, S. Oh, K.I. Park, M. Byun, H. Park, G. Ahn, C.K. Jeong, K. No, H. Kwon, S.G. Lee, B. Joung, K.J. Lee, *Adv. Mater.* 26 (2014) 4880–4887.
- [15] J.H. Lee, K.Y. Lee, M.K. Gupta, T.Y. Kim, D.Y. Lee, J. Oh, C. Ryu, W.J. Yoo, C.Y. Kang, S.J. Yoon, J.B. Yoo, S.W. Kim, *Adv. Mater.* 26 (2014) 765–769.
- [16] J. Chen, Y. Huang, N. Zhang, H. Zou, R. Liu, C. Tao, X. Fan, Z.L. Wang, *Nat. Energy* 1 (2016) 16138.
- [17] J.W. Zhong, Y. Zhang, Q.Z. Zhong, Q.Y. Hu, B. Hu, Z.L. Wang, *J. Zhou, ACS Nano* 8 (2014) 6273–6280.
- [18] D. Yang, D. Kim, S.H. Ko, A.P. Pisano, Z. Li, I. Park, *Adv. Mater.* 27 (2015) 1207–1215.
- [19] L. Zheng, Z.-H. Lin, G. Cheng, W. Wu, X. Wen, S. Lee, Z.L. Wang, *Nano Energy* 9 (2014) 291–300.
- [20] X. Chen, T. Jiang, Y. Yao, L. Xu, Z. Zhao, Z.L. Wang, *Adv. Funct. Mater.* 26 (2016) 4906–4913.
- [21] X. Chen, T. Jiang, Z.L. Wang, *Appl. Phys. Lett.* 110 (2017) 033505.
- [22] L. Zheng, Y. Wu, X. Chen, A. Yu, L. Xu, Y.S. Liu, H. Li, Z.L. Wang, *Adv. Funct. Mater.* 27 (2017) 1606408.
- [23] S. Shian, K. Bertoldi, D.R. Clarke, *Adv. Mater.* 27 (2015) 6814–6819.
- [24] S. Niu, Y. Liu, X. Chen, S. Wang, Y. Zhou, L. Lin, Y. Xie, Z.L. Wang, *Nano Energy* 12 (2015) 760–774.
- [25] T. Jiang, X. Chen, C.B. Han, W. Tang, Z.L. Wang, *Adv. Funct. Mater.* 25 (2015) 2928–2938.
- [26] D.H. Raguin, G.M. Morris, *Appl. Opt.* 32 (1993) 2582–2598.
- [27] C.H. Yang, B. Chen, J. Zhou, Y.M. Chen, Z. Suo, *Adv. Mater.* 28 (2016) 4480–4484.



Dr. Xiangyu Chen received his B.S. degree in Electrical Engineering from Tsinghua university in 2007 and his Ph.D. in Electronics Physics from Tokyo Institute of Technology in 2013. Now he is an associate professor in Beijing Institute of nanoenergy and nanosystems, Chinese Academic of Sciences. His main research interests have been focused on the field of organic electronics devices, self-powered nano energy system and the nonlinear optical laser system for characterizing the electrical properties of the devices.



Yali Wu received her B.S. degree in Electrical Engineering and Automation from GongQing college of Nanchang university in 2014, and she is currently pursuing a M.S. in Shanghai University of Electric Power. Her research interests are focused on the application of triboelectric nanogenerator.



Dr. Aifang Yu obtained her Ph.D. degree (2007) from Technical Institute of Physics and Chemistry, Chinese Academy of Science (CAS). She joined the group of Prof. Zhong Lin Wang at National Center for Nanoscience and Technology of China in 2009. In 2012, she joined Beijing Institute of Nanoenergy and Nanosystems (BINN), Chinese Academy of Sciences (CAS) as an associate professor. Her main research interests focus on the fields of nanogenerators and self-powered nanosystems.



Dr. Liang Xu received his Ph.D. degree from Tsinghua University (THU) in 2012, with awards of Excellent Doctoral Dissertation of THU and Excellent Graduate of Beijing. Before that he achieved bachelor's degree of mechanical engineering in Huazhong University of Science & Technology (HUST) in 2007. He is now a postdoctoral fellow in Beijing Institute of Nanoenergy and Nanosystems, Chinese Academy of Sciences (CAS), under the supervision of Prof. Zhong Lin Wang. His research interests include nanogenerators and self-powered nanosystems, fundamental tribological phenomena, scanning probe microscopy and molecular dynamics simulation.



Prof. Hexing Li received his Ph.D. in chemistry from Fudan University in 1998. He was appointed as an Associated Professor in the Chemistry Department at Shanghai Normal University in 1994 and promoted to a Professor in 1999. He took up joint professor positions in East China Normal University, East China Science and Technology University. His research interests are related to the design of amorphous alloy catalysts for hydrogenation, photocatalysts for degrading organic pollutants, and mesoporous organometallic catalysts for water-medium organic reactions.



Dr. Li Zheng is an associate professor in Shanghai University of Electric Power. She received her M. S. from Chinese Academy of Sciences (CAS) in 2006 and Ph.D. degree from Shanghai Jiao Tong University in 2009. Her current research interests include nanowire lasers, nanos-structure-based optoelectronic devices, nanogenerator, and self-powered nanosystems.



Prof. Zhong Lin Wang received his Ph.D. from Arizona State University in physics. He now is the Hightower Chair in Materials Science and Engineering, Regents' Professor, Engineering Distinguished Professor and Director, Center for Nanostructure Characterization, at Georgia Tech. Prof. Wang has made original and innovative contributions to the synthesis, discovery, characterization and understanding of fundamental physical properties of oxide nanobelts and nanowires, as well as applications of nanowires in energy sciences, electronics, optoelectronics and biological science. His discovery and breakthroughs in developing nanogenerators established the principle and technological roadmap for harvesting mechanical energy from the environment and biological systems for powering a personal electronics. His research on self-powered nanosystems has inspired the worldwide effort in academia and industry for studying energy for micro-nano-systems, which is now a distinct disciplinary in energy research and future sensor networks. He coined and pioneered the field of piezotronics and piezophotonics by introducing piezoelectric potential gated charge transport process in fabricating new electronic and optoelectronic devices. Details can be found at: www.nanoscience.gatech.edu.



Dr. Yongsheng Liu is a professor in Institute of Solar Energy, Shanghai University of Electric Power, and a Ph.D. supervisor in Materials Genome Institute, Shanghai University. He received his Ph.D. degree in 2006 from Shanghai University (China). His current research is focused mainly on solar cell materials, renewable energy, and magnetic materials.